FREQUENCY-TEMPERATURE ANALYSIS OF MEMS AT-CUT QUARTZ RESONATORS.

Y-K Yong[a] and J. Vig[b], A. Ballato[b], R. Kubena[c] and R. M'Closkey[d]

[a]Civil & Environmental Engineering Dept., Rutgers University, NJ, U.S.A. yyong@rci.rutgers.edu
[b]U.S. Army CECOM, [c]HRL Laboratories and [d]University of California Los Angeles

Abstract

An analytical study of the frequency-temperature behavior of MEMS AT-cut quartz resonator structures was performed. The piezoelectric, Lagrangian equations for the frequency-temperature behavior of quartz were employed[1]. Two types of resonator structures were studied: A 1 GHz rectangular plate with rectangular electrodes and a 1 GHz rectangular ring electrode mesa (REM) plate. For MEMS resonators, the REM design confers certain advantages in attaining higher resonant frequencies and lower electrode noise.

I. Introduction

The design of stable resonators is usually done by engineers with years of experience and experimentation. There is however not much experience in designing a stable quartz MEMS thickness shear resonator in the frequency range of 3 GHz because the existing conventional resonator designs will not work. A 3 GHz resonator will have an electrode to plate thickness ratio of more than 27%[2].

The frequency-temperature behavior of conventional rectangular plate quartz resonators is well known, however that of a ring electrode mesa (REM) structure is not. A possible application of MEMS AT-cut resonators would be as the reference oscillator in miniature atomic clocks and nanoresonator development programs.

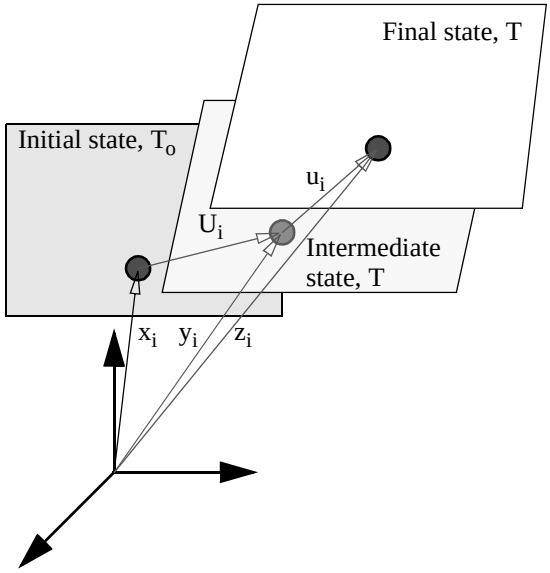

FIG. 1: Position vectors x_i, y_i and z_i of a material point at the respective initial, intermediate and final states.

II. Piezoelectric Lagrangean Equations for the Frequency-Temperature Behavior of Quartz Resonators.

We state the linear Lagrangean piezoelectric equations of small vibrations superposed on thermal deformations induced by steady, uniform temperature change in quartz which are based upon the three-dimensional mechanical equations of incremental motion superposed on homogeneous thermal strains[3]. The full details of the development of the incremental equations is not repeated here, and the interested reader is referred to reference[3]. The formulation is similar to those, for example, by Sinha and Tiersten[4], and Dulmet and Bourquin[5], but we prefer to use the Piola-Kirchhoff stress tensor of the second kind for reasons of symmetry. Figure 1 shows the three states of the resonator. The following incremental Lagrangean equations which includes the piezoelectric effect are as follows:

IIa. Strain-displacement, and electric field-potential relations.

$$s_{ij} = \frac{1}{2}(\beta_{kj}u_{k,i} + \beta_{ki}u_{k,j}) \text{, and} \tag{1}$$

$$E_i = -\phi_{,i} \text{, where} \tag{2}$$

$$\beta_{ik} = \delta_{ik} + \alpha_{ik}^{(1)}\theta + \alpha_{ik}^{(2)}\theta^2 + \alpha_{ik}^{(3)}\theta^3 \text{ and} \tag{3}$$

$$\theta = (T - T_o). \tag{4}$$

The terms s_{ij}, $u_{k,i}$, E_i and ϕ are, respectively, the incremental strains, the first partial derivative of incremental displacement, incremental electric field and incremental electric potential. δ_{ik}, $\alpha_{ik}^{(n)}$, denote the Kronecker delta and nth order temperature coefficients of thermal expansion, respectively. T and T_o are the temperatures of the intermediate state and initial (natural) state, respectively, and θ is the temperature change. The reference temperature T_o is set to 25^o C.

IIb. Equations of motion and electrostatics.

$$\beta_{ik}\sigma_{kj,j} = \rho\ddot{u}_i \text{ in } V, \text{ and} \tag{5}$$

$$D_{i,i} = 0 \text{ in } V, \tag{6}$$

where σ_{kj} is the incremental stress tensor, ρ the mass density, u_i the incremental mechanical displacement and D_k the incremental electric displacement vector.

IIc. Initial and boundary conditions.

A unique solution is guaranteed by specifying

u_i, $\dot{u}_j$, and E_j at each point of the body at an initial time $t = t_o$, and by specifying at all times one member of each of the following products on the crystal surface: p_1u_1, p_2u_2, p_3u_3, and $q\phi$ where $p_i = n_j\beta_{ik}\sigma_{kj}$ is the component of the surface traction vector, $q = n_iD_i$ is the surface charge density and n_i is the unit outward normal to the surface.

IId. Constitutive relations.

$$\sigma_{ij} = D_{ijkl}s_{kl} - e^{\theta}_{kij}E_k, \tag{7}$$

$$D_i = e^{\theta}_{ijk}s_{jk} + \varepsilon^{\theta}_{ik}E_k \tag{8}$$

$$D_{ijkl} = C_{ijkl} + D^{(1)}_{ijkl}\theta + D^{(2)}_{ijkl}\theta^2 + D^{(3)}_{ijkl}\theta^3 \tag{9}$$

$$e^{\theta}_{ijk} = e_{ijk} + e^{(1)}_{ijk}\theta + e^{(2)}_{ijk}\theta^2 + e^{(3)}_{ijk}\theta^3 \tag{10}$$

$$\varepsilon^{\theta}_{ik} = \varepsilon_{ik} + \varepsilon^{(1)}_{ik}\theta + \varepsilon^{(2)}_{ik}\theta^2 + \varepsilon^{(3)}_{ik}\theta^3 \tag{11}$$

where C_{ijkl} is the elastic stiffness tensor measured at constant electric field and temperature, $D^{(n)}_{ijkl}$ are the *n*th order thermoelastic constants, e_{ijk} is the piezoelectric stress constants tensor measured at constant strain and temperature, $e^{(n)}_{ijk}$ are the *n*th temperature coefficient of piezoelectric stress constants, ε_{ik} is the dielectric permittivity constants tensor measured at constant strain and temperature and $\varepsilon^{(n)}_{ik}$ are the *n*th temperature coefficient of dielectric permittivity constants.

III. Comparison of measured data[6] with 3-D FEM results using the Lagrangian formulation for frequency-temperature behavior.

The accuracy of the Lagrangian formulation and the material constants of quartz is demonstrated by comparing some 3-D FEM results with those of measured data by Sekimoto and his co-workers[6]. Figures 2a, 2b and 2c show the comparison of some resonant modes measured in reference 6 with the 3-D FEM results. The figures and FEM results were made by T. Imai and M. Tanaka of Seiko Epson. The comparisons are quite good. We employ the Lagrangian formulation for our analysis of the MEMS resonators.

IV. Frequency-temperature behavior of MEMS AT-cut quartz resonators.

For our present analysis of the MEMS AT-cut quartz resonators, we employ a straight-crested wave model and 2-D finite elements[2]. The immediate advantage of this 2-D modeling rather than 3-D is the problem size. We could still get salient characteristics of the MEMS resonators from the 2-D models because of the straight crested wave form of the fundamental thickness shear mode in rectangular plates[2].

IVa. Fundamental thickness shear mode shapes.

Figure 3a shows a representative rectangular ring electrode mesa resonator, while fig. 3b is the 2-D cross sectional view which is modeled using 2-D finite elements. The dimensions shown are for a nominal 1 GHz resonator. Figure 4 is the mode shape of its fundamental thickness shear mode.

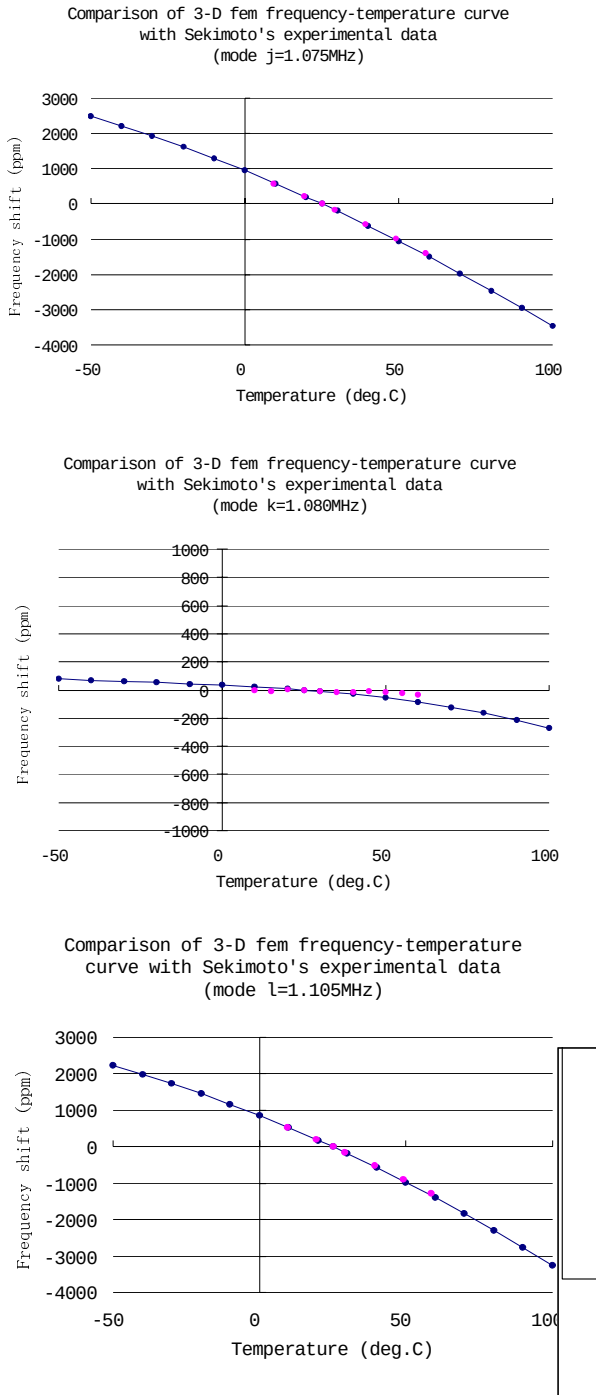

FIG. 2: For figures 2a, 2b, and 2c: Comparison of measured data[6] with 3-D FEM results (measured data are purple discrete points).

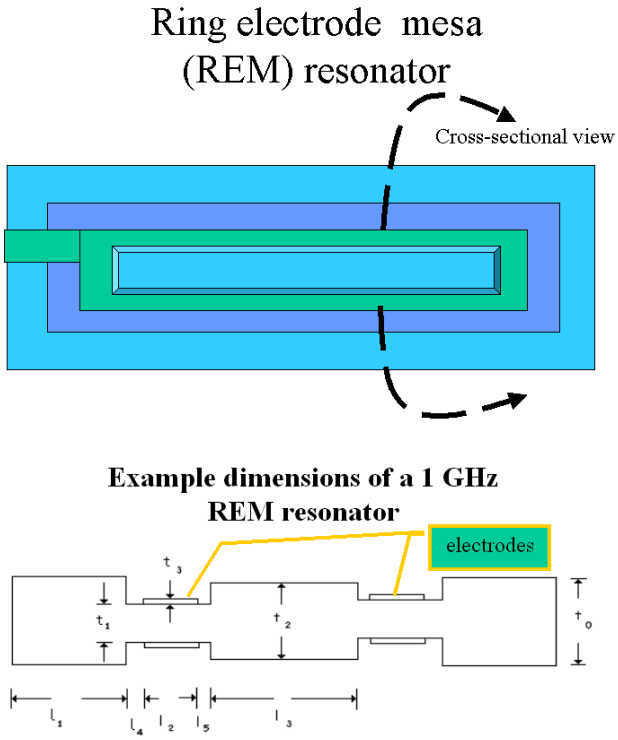

FIG. 3: Representative rectangular ring electrode mesa resonator (Fig.3a) and its 2-D straight-crested wave model for 2-D finite elements (Fig.3b).

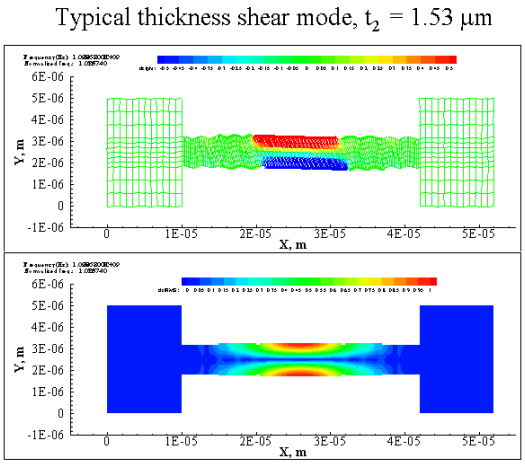

FIG. 4: Mode shape of the fundamental thickness shear mode in the REM resonator.

The REM resonator is compared with a usual mesa resonator shown below in Fig.5a along with the nominal dimensions for a 1 GHz resonator. Figure 5b is the mode shape of the fundamental thickness shear mode.

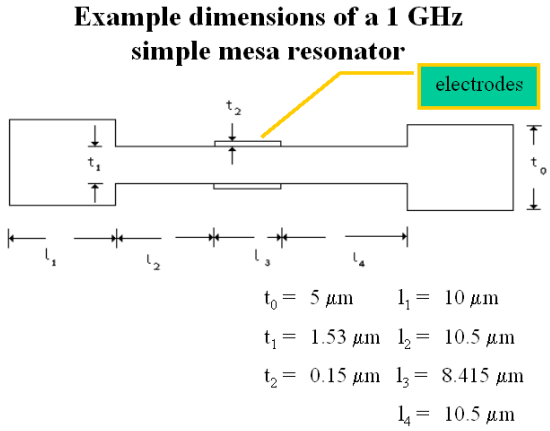

FIG. 5: 2-D model of a representative rectangular mesa resonator (Fig.5a) and its fundamental thickness shear mode shape (Fig.5b).

We note that the operating fundamental thickness shear mode shapes of the two resonators, REM and simple mesa, are essentially the same, however the electrode in the REM resonator is placed in the relatively inactive area of the energy trapped region at the center of the plate, hence noise and aging contributions due to electrodes should be less than those in the simple mesa resonator. The electrode of the REM resonator contributes less mass loading and hence higher frequency than the simple mesa resonator.

IVb. Use of frequency spectrum to select dimensions for high Q and "clean mode" resonator.

The frequency spectrum is defined in this paper as a graph of the resonant frequencies as a function of a variable of interest. Typically the variable could be the length to thickness ratio of the mesa, the length of the electrode, or the thickness/mass of the electrodes. We could use the

frequency spectrum to identify dimensional regions where high Q and “clean mode” can be obtained. The “clean mode” resonator will have no interference from spurious modes which will cause activity dips and adversely affect its frequency-temperature behavior. Figures 6a, 6b, 6c, and 6d show a series of graphs of the frequency spectrum of the REM resonator as a function the resonator length to thickness ratio with useful criteria for identifying the fundamental thickness shear mode from the “sea” of resonant modes in Fig.6a. In Fig. 6b, since the thickness shear mode has a large u_1 magnitude, modes with this characteristic are identified in blue deltas. In Fig. 6c, since the thickness shear mode has high energy trapping, modes with this characteristic are identified in red squares. Finally in Fig. 6d, since the thickness shear mode has a high surface charge, modes with low surface charges are removed. We can then see clearly that the mode of interest - fundamental thickness shear mode- is the curve identified with red squares near the bottom of the frequency spectrum.

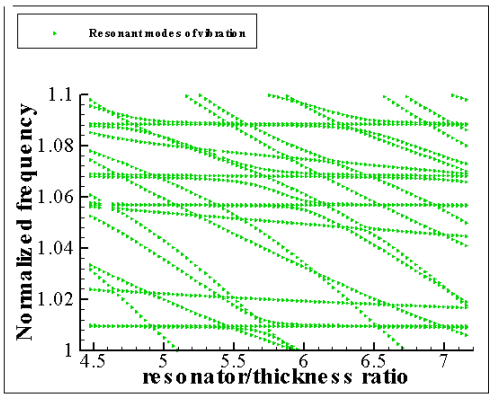

Fig. 6a

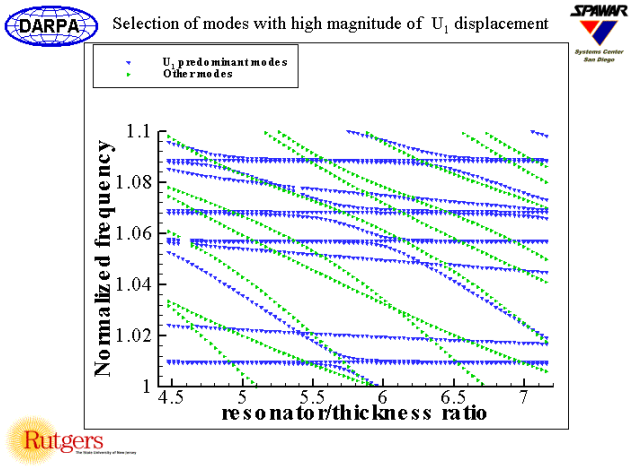

Fig. 6b

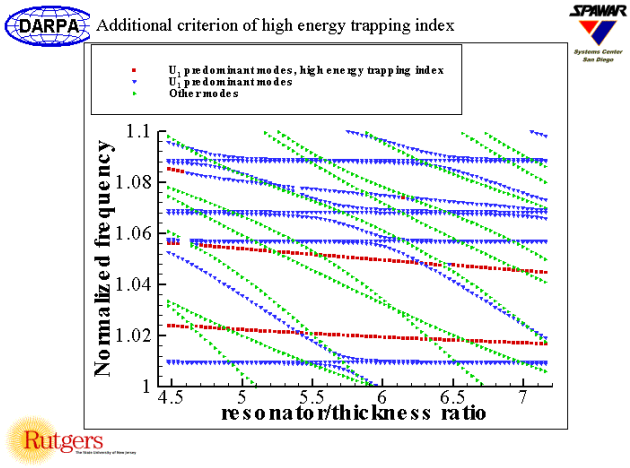

Fig. 6c

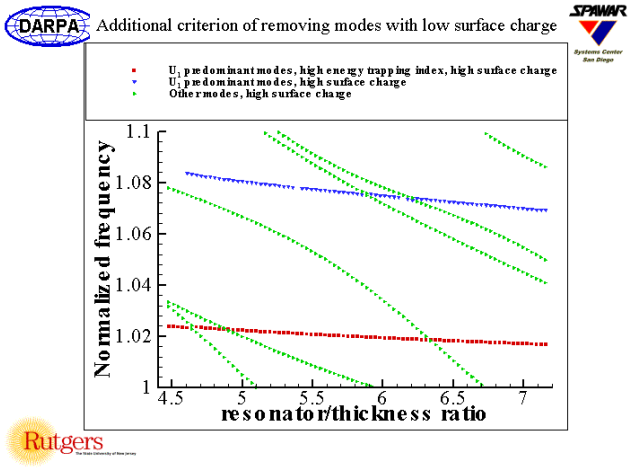

Fig. 6d.

FIG. 6: Frequency spectra of the REM resonator as a function of the resonator length to thickness ratio.

IVc. Frequency-temperature behavior of REM resonator versus simple mesa resonator.

We demonstrate the differences in the frequency-temperature behavior of REM resonator versus simple mesa resonator in a series of graphs below. In figures 7a, 7b, and 7c, the effects of different thicknesses of electrodes on, respectively, frequency-temperature behavior in parts per million, frequency-temperature behavior in hertz, and relative admittance of the resonator if the magnitude of the electric potential at the electrodes are constant are demonstrated. In Fig. 7b we observe the simple mesa resonator frequency is affected more strongly by the electrode thickness. In Fig. 7c, we see that the admittance of the REM resonator is about an order of magnitude lower than the simple mesa resonator. In Fig. 8, the effects of changing the AT-cut angle on the frequency-temperature is shown, and we observe the effects are the same for both REM and simple mesa resonators.

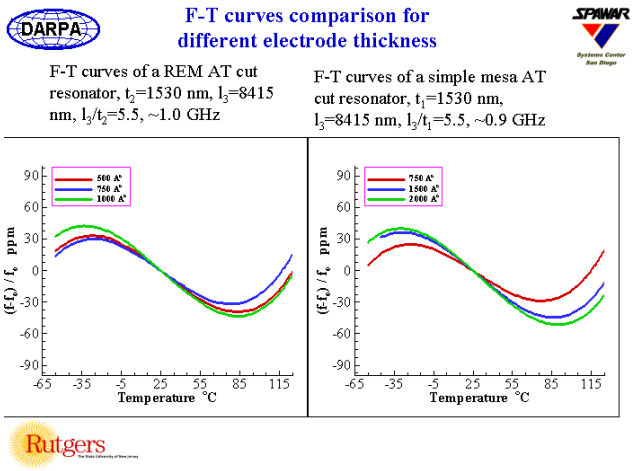

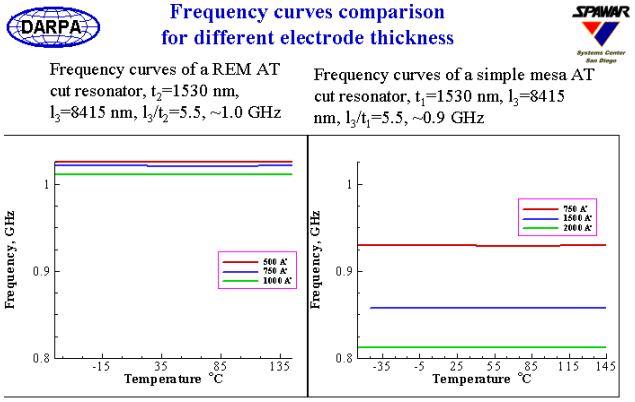

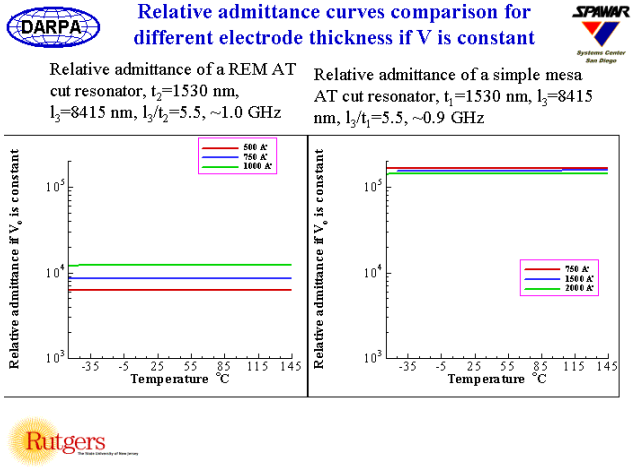

FIG. 7: Effects of the change in electrode thickness on (Fig. 7a) frequency-temperature behavior in ppm, (Fig. 7b) frequency-temperature behavior in hertz, and (Fig. 7c) relative admittance if the electric potential at the electrode is held constant.

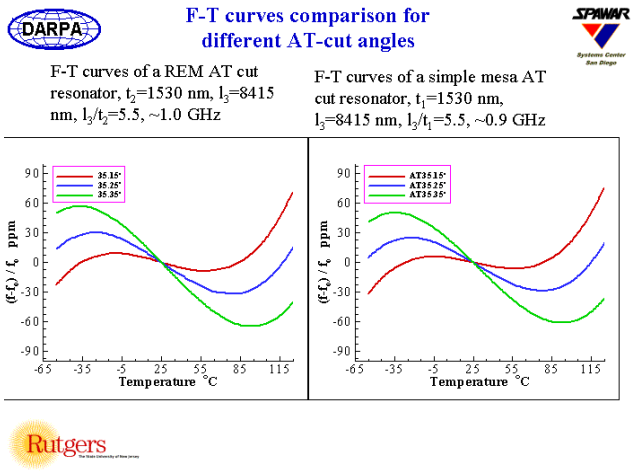

FIG. 8: Effect of changing the AT-cut angles on the frequency-temperature behavior.

V. Summary of Analysis

1. Decreasing the length to thickness ratio causes the frequency-temperature curves to behave as if the AT-cut angles are larger.
2. Increasing the electrode thickness causes the frequency-temperature curves to behave as if the cut angles are larger.
3. The REM resonator can achieve higher (10%) resonant frequencies than the simple mesa resonator. The simple mesa resonator is more sensitive to changes in electrode thickness.
4. The REM resonator has an admittance which is more than an order of magnitude less than that of a simple mesa resonator.

Acknowledgment

Support by DARPA (program director Clark Nguyen) and SPAWAR is gratefully acknowledged.

References

1. Y-K Yong and W. Wei, "Lagrangian Temperature Coefficients of the Piezoelectric Stress Constants and Dielectric Permittivity of Quartz", *Proceedings of the 2000 IEEE International Frequency Control Symposium*, 2000, pp. 420-424.
2. Y-K Yong, J. Vig and A. Ballato, "Straight Crested Wave Analysis of Quartz MEMS Ring Electroded Mesa Resonators", *Proceedings of the 2002 IEEE Ultrasonics Symposium*, 2002.
3. P.C.Y. Lee and Y-K. Yong, "Frequency-Temperature Behavior of Thickness Vibrations of Doubly Rotated Quartz Plates Affected by Plate Dimensions and Orientations", *Journal of Applied Physics*, 60(7), 1986, pp. 2327-2342.
4. B. K. Sinha and H. F. Tiersten, "First Temperature Derivatives of the Fundamental Elastic Constants of Quartz", *Journal of Applied Physics*, 50(4), 1979, pp. 2732-2739.
5. B. Dulmet and R. Bourquin, "Application of Lagrangian Effective Material Constants to the Study of the Thermal Behavior of SAW Propagation in Piezoelectric Crystals", *Proceedings of the 1994 IEEE Ultrasonics Symposium*, 1994, pp. 331-336.
6. H. Sekimoto, S. Goka, A. Ishizaki and Y. Watanabe, "Frequency-Temperature of Spurious Vibrations of Rectangular AT-Cut Quartz Plates", *Proceedings of the IEEE International Frequency Control Symposium*, 1997, pp. 710-714.